

- 2572 (1975); (b) T. Sakurai, O. Yamauchi, and A. Nakahara, *ibid.*, **49**, 169 (1976); (c) *ibid.*, **49**, 1579 (1976); (d) *J. Chem. Soc., Chem. Commun.*, 553 (1976); (e) O. Yamauchi, T. Sakurai, and A. Nakahara, *Bull. Chem. Soc. Jpn.*, **50**, 1776 (1977).
- (36) T. Sakurai, O. Yamauchi, and A. Nakahara, *J. Chem. Soc., Chem. Commun.*, 718 (1977).
- (37) In the previous communication³⁶ the modification crystallized from aqueous methanol (or ethanol) and dried in the open air was described as $n = 0.25$. However, the X-ray analysis of this complex⁴⁹ revealed that it is anhydrous, and our elemental analysis data are compatible with the values calculated for the complex with $n = 0$. Therefore, we now express this modification as an anhydrous complex. Drying in the open air, however, might have affected the elemental analysis owing to the moisture on the crystals. On the other hand, thermal analysis of the tetrahydrate afforded the weight loss corresponding to $3.70\text{H}_2\text{O}$, with the ΔH value of 54 kcal/mol based on the value of 26.51 kcal/mol for the dehydration $\text{CuSO}_4 \cdot 5\text{H}_2\text{O} \rightarrow \text{CuSO}_4 \cdot 3\text{H}_2\text{O} + 2\text{H}_2\text{O}$. Since the X-ray structure analysis confirmed the presence of four molecules of water, the result seems to indicate partial loss of water during storage.
- (38) Personal communication from Professor Y. Sasada of Tokyo Institute of Technology.
- (39) A. Albert and E. P. Serjeant, "Ionization Constants of Acids and Bases", Methuen, London, 1962.
- (40) A. W. Herlinger, S. L. Wenhold, and T. V. Long, II, *J. Am. Chem. Soc.*, **92**, 6474 (1970).
- (41) I. G. Sayce, *Talanta*, **15**, 1397 (1968).
- (42) A. E. Martell and R. M. Smith, "Critical Stability Constants", Vol. 1, Plenum Press, New York, 1974.
- (43) L. D. Pettit and J. L. M. Swash, *J. Chem. Soc., Dalton Trans.*, 2416 (1976).
- (44) V. S. Sharma and J. Schubert, *J. Chem. Educ.*, **46**, 506 (1969).
- (45) Although the log β values for the protonated complex have been reported by several groups of workers,^{11,14-16} inclusion of the species usually resulted in poor convergence in our calculation, and we accordingly neglected it. In this connection, Brookes and Pettit¹⁶ also reported that for the systems Cu(II)-L- or $\text{D-histidine-amino acid}$ it was always of minor importance and absent in some cases.
- (46) J. M. Tsangaris and R. B. Martin, *J. Am. Chem. Soc.*, **92**, 4255 (1970).
- (47) R. B. Martin and R. Prados, *J. Inorg. Nucl. Chem.*, **36**, 1665 (1974).
- (48) G. Brookes and L. D. Pettit, *J. Chem. Soc., Chem. Commun.*, 385 (1975).
- (49) T. Ono, H. Shimanouchi, Y. Sasada, T. Sakurai, O. Yamauchi, and A. Nakahara, *Bull. Chem. Soc. Jpn.*, in press.
- (50) F. S. Stephens, R. S. Vagg, and P. A. Williams, *Acta Crystallogr., Sect. B*, **31**, 841 (1975).
- (51) According to the personal communication from Professor Y. Sasada, newly prepared $\text{Cu(L-Ala)(L-His) \cdot 4H}_2\text{O}$ was disclosed by X-ray analysis to have a cis arrangement with the histidine carboxyl group hydrogen bonded to the apically coordinated water molecule.
- (52) Recent NMR studies on the corresponding ternary complexes of palladium(II) provide evidence in support of the intramolecular ligand-ligand interactions (O. Yamauchi and A. Odani, results partly presented at the ACS/CSJ Chemical Congress, Honolulu, April 1979). From the comparison of the spectral patterns of the systems, such as $\text{Pd(L- or D-His)(L-AA)}$ ($\text{AA} = \text{Hmser}$ or Gln), Pd(Ha)(L-AA) ($\text{Ha} = \text{histamine}$), Pd(L-Ala)(L-AA) , and Pd(L-AA)_2 , the spectral patterns of coordinated L-AA have been found to be affected by the presence of the carboxylate group of histidine. The result indicates the conformational change of L-AA due to the interaction with the carboxylate group, and further points to similar interactions in the copper(II) complexes, since both Cu(II) and Pd(II) prefer a square-planar structure and the apical bonding present in Cu(II) but probably absent in Pd(II) is not supposed to interrupt the intramolecular ligand-ligand interaction.

Structure of a 12-Vertex Arachno Carborane, $\sigma\text{-(}\eta^5\text{-C}_5\text{H}_5\text{)Co(}\eta^5\text{-C}_5\text{H}_4\text{)}^+\text{-(CH}_3\text{)}_4\text{C}_4\text{B}_8\text{H}_8^-$, an Analogue of $\text{B}_{12}\text{H}_{12}^{6-}$ and $\text{C}_2\text{B}_{10}\text{H}_{12}^{4-}$. Mechanisms of Carborane Fluxional Behavior and Metallocarborane Formation from the $(\text{CH}_3)_4\text{C}_4\text{B}_8\text{H}_8^{2-}$ Ion¹

Russell N. Grimes,* J. Robert Pival, and Ekk Sinn

Contribution from the Department of Chemistry, University of Virginia, Charlottesville, Virginia 22901. Received February 20, 1979

Abstract: The structure of the title compound, the first confirmed example of a 12-vertex arachno borane cage, was determined by single-crystal X-ray diffraction and is formulated as a cobaltocenium-substituted derivative of the $(\text{CH}_3)_4\text{C}_4\text{B}_8\text{H}_9^-$ ion, which in turn is obtained by protonation of the $(\text{CH}_3)_4\text{C}_4\text{B}_8\text{H}_8^{2-}$ dianion. The carborane polyhedron, a 30-electron, 12-vertex cage, has an open basket-like geometry in which the four C-CH₃ groups occupy contiguous positions on the open face. One of the C-CH₃ units is coordinated to only two framework atoms, and the "extra" hydrogen atom is attached to this bridging carbon. The methyl group on the bridging carbon atom is located over the open face of the cage, and the cobaltocenium substituent is attached to a boron atom on the open face adjacent to the bridging carbon. From this structure and the previously determined geometry of neutral $(\text{CH}_3)_4\text{C}_4\text{B}_8\text{H}_8$, a mechanism is proposed for the formation of the dianion and for its fluxional behavior in solution. Based on this mechanism, a scheme is proposed to account for the formation of several tetracarboranes from the $(\text{CH}_3)_4\text{C}_4\text{B}_8\text{H}_8^{2-}$ dianion. The interconversion of neutral $(\text{CH}_3)_4\text{C}_4\text{B}_8\text{H}_8$ isomers and the probable structure and fluxionality of isomer B are discussed. The $\sigma\text{-(C}_5\text{H}_5\text{)Co(C}_5\text{H}_4\text{)}^+\text{-(CH}_3\text{)}_4\text{C}_4\text{B}_8\text{H}_8^-$ molecule crystallizes in the triclinic $\overline{1}1$ space group with $a = 8.047$ (3) Å, $b = 37.05$ (2) Å, $c = 21.551$ (9) Å, $\alpha = 90.04$ (6)°, $\beta = 97.13$ (8)°, $\gamma = 89.94$ (7)°, and $V = 6375$ (3) Å³; $R = 0.047$ for the 7516 reflections for which $F_o^2 > 3 \sigma(F_o^2)$. There are 12 molecules in the unit cell and three molecules per asymmetric unit. Full-matrix least-squares refinement of the positional and thermal parameters of all 168 atoms (including all hydrogens) in the asymmetric unit gave a final R value of 0.047.

The stability of the icosahedron as a structural unit in boron chemistry is well known.² Molecular orbital calculations^{3,4} on the $\text{B}_{12}\text{H}_{12}^{2-}$ ion indicate the presence of 13 bonding molecular orbitals, which is precisely the number of bonding electron pairs that are available for linking the 12 BH units in that species. The icosahedral carborane isomers, 1,2-, 1,7-, and 1,12- $\text{C}_2\text{B}_{10}\text{H}_{12}$, are isoelectronic with $\text{B}_{12}\text{H}_{12}^{2-}$ and similarly contain 26 skeletal electrons in 13 bonding MOs exclusive of C-H and B-H bonding.²

If an electron pair is added to any of these filled-shell icosahedral systems, forming 28-electron $\text{B}_{12}\text{H}_{12}^{4-}$, $\text{C}_2\text{B}_{10}\text{H}_{12}^{2-}$, or $\text{C}_4\text{B}_8\text{H}_{12}$ species, one expects distortion of the polyhedral framework; however, it is now clear that the nature of this distortion can, and does, vary widely in different systems. Although the prototype borane $\text{B}_{12}\text{H}_{12}^{4-}$ is unknown and the structures of the $\text{C}_2\text{B}_{10}\text{H}_{12}^{2-}$ isomers have not been established, X-ray diffraction studies of the 28-electron⁵ species $\text{R}_2\text{C}_2\text{B}_{10}\text{H}_{11}^-$ ($\text{R} = \text{CH}_3^6$ or C_6H_5^7), $(\text{CH}_3)_4\text{C}_4\text{B}_8\text{H}_8$,⁸ ($\eta^5\text{-}$

C₅H₅)Fe(CH₃)₄C₄B₇H₈⁹, (η^5 -C₅H₅)₂Co₂C₄B₆H₁₀ (isomer VII),¹⁰ (η^5 -C₅H₅)₂Co₂(CH₃)₄C₄B₆H₆ (isomer V),¹¹ (η^5 -C₅H₅)Co(CH₃)₄C₄B₇H₆-OC₂H₅,¹² and (η^5 -C₅H₅)Co(CH₃)₄C₄B₇H₇ (isomer II)¹³ have been conducted. The cage geometries in these molecules fall into several distinct classes in which the deviation from icosahedral geometry ranges from mild to severe.¹²

Addition of yet another pair of electrons to create a 30-electron 12-vertex species analogous to B₁₂H₁₂⁶⁻ should, in principle,⁵ produce an even more open (arachno)¹⁴ framework. Neither B₁₂H₁₂⁶⁻ nor its dicarbon carborane analogue C₂B₁₀H₁₂⁴⁻ is known, but the corresponding tetracarbon system, C₄B₈H₁₂²⁻, exists in the form of a C-tetramethyl derivative; the (CH₃)₄C₄B₈H₈²⁻ dianion is easily obtained by reduction of the neutral species (CH₃)₄C₄B₈H₈ with sodium in tetrahydrofuran.⁹ Although we have prepared and structurally characterized a number of transition-metal complexes of (CH₃)₄C₄B₈H₈²⁻, the geometry of the ion itself has remained a mystery despite repeated attempts to produce salts suitable for crystallographic analysis.

In this paper we report the crystal structure of a cobaltocenium-substituted derivative^{1b} of the dianion, which provides the first established example of a 12-vertex arachno borane system. In addition, the solution of this structure allows us for the first time to make some sense of the peculiar metallocarborane structures which are obtained by metal insertion into the (CH₃)₄C₄B₈H₈²⁻ ion,^{1b,9} and to formulate possible mechanisms for the metal insertion processes.

Experimental Section

A sample of (C₅H₅)Co(C₅H₄)-(CH₃)₄C₄B₈H₈ was prepared from (CH₃)₄C₄B₈H₈ by reduction to the anion and treatment with CoCl₂, NaC₅H₅, and HCl as described elsewhere.^{1b} A purple crystal, grown by vapor diffusion of pentane into a methylene chloride solution, was mounted on a glass fiber in an arbitrary orientation and examined by precession photography, which indicated good crystal quality. Crystal data: CoC₁₈B₈H₂₉, mol wt 391; space group *I*1; *a* = 8.047 (3) Å, *b* = 37.05 (2) Å, *c* = 21.551 (9) Å; α = 90.04 (6)°, β = 97.13 (8)°, γ = 89.94 (7)°; *V* = 6375 (3) Å³; *Z* = 12; μ (Mo K α) = 8.4 cm⁻¹; ρ_{calcd} = 1.22 g cm⁻³; crystal dimensions (distances in mm from centroid): (100) 0.22, ($\bar{1}20$) 0.23, ($\bar{1}2\bar{2}$) 0.20, ($\bar{1}22$) 0.20, (010) 0.125, (0 $\bar{1}0$) 0.125, (011) 0.16, (0 $\bar{1}1$) 0.16, (0 $\bar{1}\bar{1}$) 0.16, (0 $\bar{1}1$) 0.16.

For this crystal the Enraf-Nonius program SEARCH was used to obtain 25 accurately centered reflections which were then employed in the program INDEX to obtain an orientation matrix for data collection and also to provide approximate cell constants. Refined cell dimensions and their estimated standard deviations were obtained from least-squares refinement of 25 accurately centered reflections. The mosaicity of the crystal was examined by the ω scan technique and found to be satisfactory. The *I*1 setting of the unit cell was chosen because of the apparent monoclinic unit cell angles. However, no evidence of monoclinic or higher symmetry was observed in precession photographs, in diffractometer-measured reflection photographs, or in the molecular packing in the cell. Thus, there are three complete molecules with a total of 168 atoms (including hydrogens) in the asymmetric unit, and 12 molecules in the unit cell.

Collection and Reduction of the Data. Diffraction data were collected at 295 K on an Enraf-Nonius four-circle CAD-4 diffractometer controlled by a PDP8/M computer, using Mo K α radiation from a highly oriented graphite crystal monochromator. The θ - 2θ scan technique was used to record the unique intensities for all reflections for which $1^\circ < 2\theta < 45.00^\circ$. Scan widths (SW) were calculated from the formula $SW = A + B \tan \theta$ where *A* is estimated from the mosaicity of the crystal and *B* allows for the increase in the width of each peak due to K α_1 and K α_2 splitting. The values of *A* and *B*, respectively, were 0.60 and 0.35°. This calculated scan angle was extended at each side by 25% for background determination (BG1 and BG2). The net count (NC) was then calculated as $NC = TOT - 2(BG1 + BG2)$ where TOT is the estimated peak intensity. Reflection data were considered insignificant if the intensities registered less than ten counts above background on a rapid prescan, such reflections being rejected automatically by the computer. The intensities of four standard reflections were monitored at 100-reflection intervals and showed no

systematic trends. The raw intensity data were corrected for Lorentz-polarization effects and absorption (maximum and minimum transmission coefficients 0.93 and 0.66), and their standard deviations were calculated in the usual manner from counting statistics ($\rho = 0.03$).¹⁵ This produced 8165 reflections of which 7516 had $F_o^2 > 3\sigma(F_o^2)$. Only those reflections for which $F_o^2 > 3\sigma(F_o^2)$ were used in the refinement of the structural parameters.

Solution and Refinement of the Structure. The cobalt positions were determined from a three-dimensional Patterson map. Refinement of these positions phased the data sufficiently well to permit location of all remaining nonhydrogen and some hydrogen atoms from Fourier difference maps.

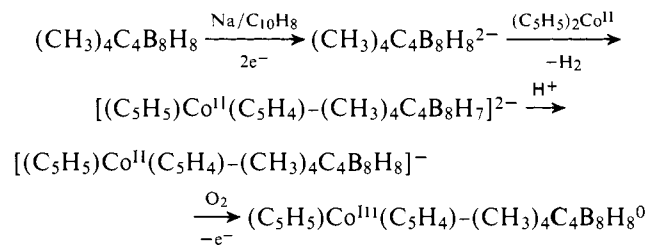
Full-matrix least-squares refinement was based on *F*, and the function minimized was $\sum w(|F_o| - |F_c|)^2$. The weights *w* were taken as $[2F_o/\sigma(F_o^2)]^2$, where $|F_o|$ and $|F_c|$ are the observed and calculated structure factor amplitudes. The atomic scattering factors for nonhydrogen atoms were taken from Cromer and Waber¹⁶ and those for hydrogen from Stewart et al.¹⁷ The effects of anomalous dispersion for all nonhydrogen atoms were included in *F_c* using Cromer and Ibers¹⁸ values for $\Delta F'$ and $\Delta F''$. Agreement factors are defined as $R = \sum ||F_o| - |F_c|| / \sum |F_o|$ and $R_w = (\sum w(|F_o| - |F_c|)^2 / \sum w|F_o|^2)^{1/2}$.

Anisotropic temperature factors were introduced for all nonhydrogen atoms. Further Fourier difference maps revealed the locations of all but seven of the 87 hydrogen atoms in the asymmetric unit; those of the remaining seven were inserted in their calculated positions and the refinement was continued to convergence, giving final values of $R = 0.047$ and $R_w = 0.062$. Owing to the large number of parameters, the refinement was conducted in sections with some parameters held fixed in any given cycle. During the last cycle of refinement, no parameter shifted more than 0.01 times its standard deviation. The computing system and programs used are described elsewhere.¹⁹ A table of structure factors is available (see paragraph at end of paper regarding supplementary material).

Results and Discussion

Final positional parameters are given in Table I while Tables II and III contain intramolecular distances and angles. Anisotropic thermal parameters are included in the supplementary material. The digits in parentheses in the tables are the estimated standard deviations in the least significant figure quoted and were derived from the inverse matrix of the last cycles of least-squares refinement calculations. Table IV lists selected mean planes in the molecule. There are no intermolecular contacts less than 3.55 Å (nonhydrogen atoms). The molecular parameters given in Tables II-IV are for molecule 1; the corresponding parameters in molecules 2 and 3 are the same as those in 1 within two standard deviations. Figures 1 and 2 are stereoviews of the structure, and Figure 3 is a diagram of the unit cell packing.

Description of the Structure. The three crystallographically independent molecules are statistically identical, as noted above. The σ -(C₅H₅)Co(C₅H₄)⁺-(CH₃)₄C₄B₈H₈⁻ zwitterion is a cobaltocenium-substituted derivative of the (CH₃)₄C₄B₈H₉⁻ monoanion, which is itself formed by protonation of (CH₃)₄C₄B₈H₈²⁻; this formulation agrees very well with the method of synthesis,^{1b} which involved treatment of (CH₃)₄C₄B₈H₈²⁻ with CoCl₂, Na⁺C₅H₅⁻, and HCl in THF solution. The sequence of formation is assumed to be



As noted earlier, cobaltacarboranes are also formed in this reaction.^{1b}

The cage structure can be described as an 11-vertex C₃B₈

Table I. Positional Parameters and Their Estimated Standard Deviations for $(C_5H_5)Co(C_5H_4)(CH_3)_4C_4B_8H_8^a$

atom	X	Y	Z	atom	X	Y	Z
Co(1)	0.021 95(9)	0.237 57(2)	0.397 61(3)	H(101)	0.112(7)	0.361(2)	0.168(3)
Co(2)	0.058 01(9)	0.317 61(2)	0.842 50(3)	H(102)	-0.138(6)	0.359(1)	0.254(2)
Co(3)	0.204 48(9)	0.580 04(2)	0.944 85(3)	H(103)	0.077(6)	0.421(1)	0.260(2)
B(101)	0.1443(8)	0.3614(2)	0.2143(3)	H(104)	0.414(6)	0.398(1)	0.239(2)
B(102)	-0.0053(8)	0.3542(2)	0.2678(3)	H(105)	0.419(6)	0.328(1)	0.213(2)
B(103)	0.1200(8)	0.3948(2)	0.2683(3)	H(106)	0.075(6)	0.294(1)	0.223(2)
B(104)	0.3207(8)	0.3816(2)	0.2534(3)	H(107)	-0.042(6)	0.315(1)	0.389(2)
B(105)	0.3243(8)	0.3355(2)	0.2422(3)	H(111)	0.368(6)	0.288(1)	0.323(2)
B(106)	0.1247(7)	0.3187(2)	0.2501(3)	H(107A)	0.142(6)	0.327(1)	0.465(2)
B(111)	0.2868(8)	0.3139(2)	0.3117(3)	H(107B)	0.179(6)	0.367(1)	0.471(2)
B(112)	0.0772(7)	0.3166(1)	0.3280(3)	H(107C)	0.291(7)	0.341(1)	0.435(2)
C(107)	0.0685(6)	0.3486(1)	0.3781(2)	H(108A)	0.045(7)	0.439(1)	0.347(2)
C(108)	0.1033(7)	0.3838(1)	0.3445(2)	H(108B)	-0.102(8)	0.414(2)	0.356(3)
C(109)	0.2855(6)	0.3884(1)	0.3303(2)	H(108C)	0.062(7)	0.414(1)	0.420(3)
C(110)	0.3804(6)	0.3528(1)	0.3172(2)	H(109A)	0.490(6)	0.426(1)	0.336(2)
CM(107)	0.1805(7)	0.3451(1)	0.4398(2)	H(109B)	0.415(7)	0.412(2)	0.406(3)
CM(108)	0.0240(8)	0.4155(1)	0.3734(3)	H(109C)	0.315(8)	0.444(2)	0.348(3)
CM(109)	0.3846(8)	0.4194(2)	0.3617(3)	H(110A)	0.631(8)	0.373(2)	0.342(3)
CM(110)	0.5681(7)	0.3518(2)	0.3424(3)	H(110B)	0.624(8)	0.326(2)	0.331(3)
CP(113)	-0.0339(6)	0.2819(1)	0.3373(2)	H(110C)	0.577(8)	0.352(2)	0.386(3)
CP(114)	-0.1491(7)	0.2778(1)	0.3834(2)	H(114)	-0.158(6)	0.297(1)	0.413(2)
CP(115)	-0.2290(6)	0.2434(1)	0.3761(3)	H(115)	-0.340(7)	0.237(1)	0.400(2)
CP(116)	-0.1614(7)	0.2254(1)	0.3280(3)	H(116)	-0.190(7)	0.203(1)	0.312(3)
CP(117)	-0.0414(7)	0.2481(1)	0.3049(2)	H(117)	0.027(6)	0.241(1)	0.271(2)
CP(118)	0.2522(7)	0.2134(2)	0.4065(3)	H(118)	0.314(9)	0.211(2)	0.370(3)
CP(119)	0.2573(7)	0.2459(1)	0.4418(3)	H(119)	0.323(6)	0.264(1)	0.430(2)
CP(120)	0.1420(8)	0.2425(2)	0.4862(2)	H(120)	0.125(8)	0.256(2)	0.517(3)
CP(121)	0.0685(8)	0.2085(2)	0.4789(3)	H(121)	-0.025(7)	0.200(1)	0.502(3)
CP(122)	0.1337(8)	0.1906(1)	0.4302(3)	H(122)	0.105(7)	0.165(1)	0.413(2)
B(201)	-0.2175(8)	0.2878(2)	0.5650(3)	H(201)	-0.204(7)	0.265(1)	0.539(2)
B(202)	-0.0378(8)	0.3111(2)	0.6027(3)	H(202)	0.088(6)	0.307(1)	0.587(2)
B(203)	-0.1851(8)	0.3320(2)	0.5417(3)	H(203)	-0.161(5)	0.341(1)	0.499(2)
B(204)	-0.3857(8)	0.3178(2)	0.5540(3)	H(204)	-0.498(6)	0.321(1)	0.520(2)
B(205)	-0.3698(8)	0.2892(2)	0.6177(3)	H(205)	-0.476(6)	0.269(1)	0.614(2)
B(206)	-0.1590(8)	0.2842(2)	0.6473(3)	H(206)	-0.108(7)	0.258(1)	0.673(2)
B(211)	-0.2862(7)	0.3125(2)	0.6854(3)	H(207)	0.065(6)	0.370(1)	0.668(2)
B(212)	-0.0713(7)	0.3224(1)	0.6894(2)	H(211)	-0.353(5)	0.306(1)	0.731(2)
C(207)	-0.0552(6)	0.3635(1)	0.6659(2)	H(207A)	-0.073(6)	0.395(1)	0.742(2)
C(208)	-0.1230(6)	0.3641(1)	0.5964(2)	H(207B)	-0.244(6)	0.389(1)	0.705(2)
C(209)	-0.3139(6)	0.3594(1)	0.5823(2)	H(207C)	-0.124(6)	0.420(1)	0.684(2)
C(210)	-0.3978(6)	0.3350(1)	0.6297(2)	H(208A)	-0.078(7)	0.390(1)	0.515(2)
CM(207)	-0.1326(7)	0.3923(1)	0.7021(2)	H(208B)	-0.052(7)	0.415(1)	0.586(3)
CM(208)	-0.0439(7)	0.3943(1)	0.5629(2)	H(208C)	0.074(8)	0.382(2)	0.559(3)
CM(209)	-0.4126(8)	0.3901(2)	0.5512(3)	H(209A)	-0.536(8)	0.379(2)	0.536(3)
CM(210)	-0.5711(7)	0.3474(2)	0.6432(3)	H(209B)	-0.414(8)	0.408(2)	0.580(3)
CP(213)	0.0616(6)	0.3097(1)	0.7457(2)	H(209C)	-0.361(8)	0.390(2)	0.511(3)
CP(214)	0.2032(6)	0.3307(1)	0.7751(2)	H(210A)	-0.650(8)	0.348(2)	0.595(3)
CP(215)	0.2950(6)	0.3100(2)	0.8225(2)	H(210B)	-0.610(7)	0.330(1)	0.669(2)
CP(216)	0.2138(7)	0.2768(1)	0.8257(2)	H(210C)	-0.568(7)	0.369(2)	0.669(3)
CP(217)	0.0709(7)	0.2767(1)	0.7803(2)	H(214)	0.236(6)	0.356(1)	0.765(2)
CP(218)	-0.1556(7)	0.3106(2)	0.8825(3)	H(215)	0.422(6)	0.315(1)	0.844(2)
CP(219)	-0.0145(8)	0.3105(2)	0.9291(2)	H(216)	0.229(7)	0.260(1)	0.852(2)
CP(220)	0.0666(8)	0.3438(2)	0.9265(3)	H(217)	-0.007(5)	0.256(1)	0.774(2)
CP(221)	-0.0204(8)	0.3645(1)	0.8790(3)	H(218)	-0.229(7)	0.292(1)	0.874(2)
CP(222)	-0.1599(7)	0.3441(1)	0.8518(2)	H(219)	0.018(7)	0.288(1)	0.954(2)
B(301)	0.3563(8)	0.4262(2)	0.8507(3)	H(220)	0.160(6)	0.352(1)	0.946(2)
B(302)	0.1850(8)	0.4567(2)	0.8346(3)	H(221)	0.009(8)	0.385(2)	0.869(3)
B(303)	0.2883(8)	0.4367(2)	0.7736(3)	H(222)	-0.236(6)	0.350(1)	0.821(2)
B(304)	0.5049(8)	0.4356(2)	0.8001(3)	H(301)	0.339(7)	0.400(1)	0.868(2)
B(305)	0.5348(8)	0.4534(2)	0.8757(3)	H(302)	0.044(6)	0.446(1)	0.831(2)
B(306)	0.3398(8)	0.4656(2)	0.8975(3)	H(303)	0.232(6)	0.420(1)	0.738(2)
C(307)	0.2050(6)	0.5149(1)	0.7880(2)	H(304)	0.593(7)	0.417(1)	0.782(2)
C(308)	0.2397(6)	0.4803(1)	0.7519(2)	H(305)	0.644(6)	0.443(1)	0.900(2)
B(311)	0.4727(7)	0.4991(2)	0.8737(3)	H(306)	0.301(7)	0.467(1)	0.947(2)
B(312)	0.2544(7)	0.5058(1)	0.8610(3)	H(307)	0.088(6)	0.519(1)	0.779(2)
C(309)	0.4247(6)	0.4711(1)	0.7524(2)	H(311)	0.556(7)	0.517(1)	0.907(2)
C(310)	0.5448(6)	0.4822(1)	0.8125(2)	H(307A)	0.276(6)	0.550(1)	0.716(2)
CM(307)	0.2893(7)	0.5474(1)	0.7624(2)	H(307B)	0.245(7)	0.569(1)	0.776(2)
				H(307C)	0.407(6)	0.546(1)	0.773(2)
				H(308A)	0.140(6)	0.504(1)	0.667(2)
				H(308B)	0.156(7)	0.457(1)	0.665(2)
				H(308C)	0.007(7)	0.474(2)	0.700(3)

Table I. (Continued)

atom	X	Y	Z	atom	X	Y	Z
CM(308)	0.1271(8)	0.4790(1)	0.6899(2)	H(309A)	0.488(8)	0.499(2)	0.674(3)
CM(309)	0.4940(8)	0.4710(2)	0.6899(3)	H(309B)	0.442(7)	0.452(2)	0.667(3)
CM(310)	0.7209(7)	0.4954(2)	0.8009(3)	H(309C)	0.607(7)	0.460(1)	0.696(3)
CP(313)	0.1559(6)	0.5278(1)	0.9082(2)	H(310A)	0.786(7)	0.474(1)	0.776(2)
CP(314)	0.0215(6)	0.5529(1)	0.8916(2)	H(310B)	0.782(7)	0.502(1)	0.844(2)
CP(315)	-0.0380(6)	0.5667(1)	0.9465(3)	H(310C)	0.700(7)	0.520(1)	0.779(2)
CP(316)	0.0613(7)	0.5513(1)	0.9976(2)	H(314)	-0.019(6)	0.557(1)	0.848(2)
CP(317)	0.1820(7)	0.5283(1)	0.9756(2)	H(315)	-0.157(7)	0.580(1)	0.943(2)
CP(318)	0.3246(8)	0.6199(1)	0.9994(3)	H(316)	0.067(7)	0.552(1)	1.033(2)
CP(319)	0.4412(7)	0.5964(1)	0.9760(3)	H(317)	0.274(6)	0.515(1)	1.001(2)
CP(320)	0.4123(7)	0.5982(1)	0.9097(2)	H(318)	0.306(7)	0.623(1)	1.052(2)
CP(321)	0.2787(8)	0.6217(1)	0.8928(3)	H(319)	0.520(6)	0.582(1)	0.997(2)
CP(322)	0.2224(8)	0.6352(1)	0.9479(3)	H(320)	0.485(7)	0.580(1)	0.890(2)
				H(321)	0.239(8)	0.631(2)	0.852(3)
				H(322)	0.137(7)	0.651(1)	0.944(2)

^a Cobalt atoms in the three independent molecules are designated Co(1), Co(2), and Co(3), respectively. Other than cobalt, atoms in molecules 1, 2, and 3 are designated by the first digit in the atom label; the last two digits indicate the location within the molecule, based on the cage numbering scheme in Figure 1. Thus, C(107) is atom C(7) in molecule 1. Methyl and cyclopentadienyl carbon atoms are labeled CM and CP, respectively.

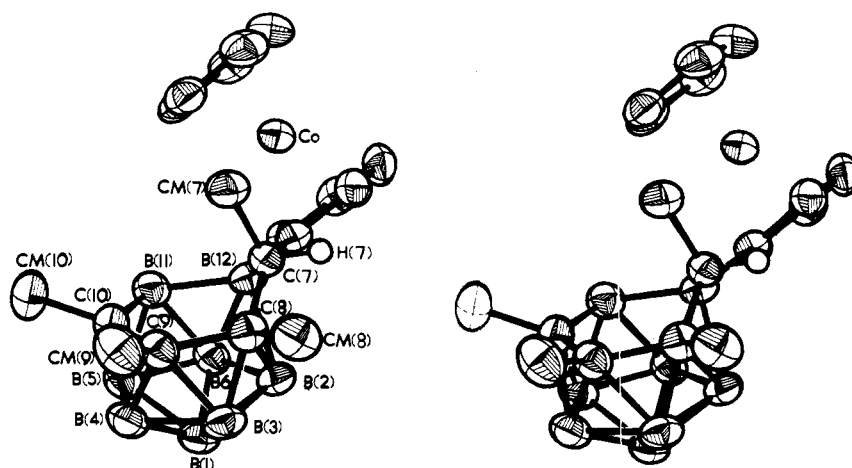


Figure 1. Stereoview of the $[(\eta^5\text{-C}_5\text{H}_5)\text{Co}(\eta^5\text{-C}_5\text{H}_4)]^+ - [(\text{CH}_3)_4\text{C}_4\text{B}_8\text{H}_8]^-$ molecule showing the cage numbering system. H atoms omitted except for H(7).

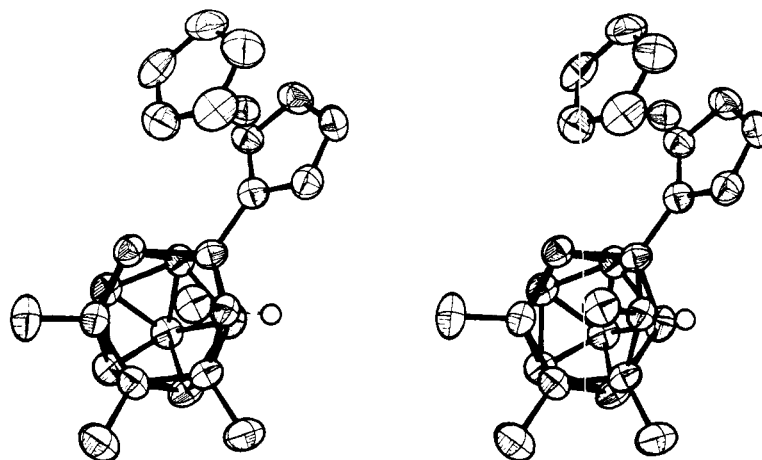


Figure 2. View from above the open face.

distorted icosahedral fragment in which the B(12)-C(8) edge on the open face is stretched to a nonbonding distance [2.522 (5) Å] with B(12) and C(8) bridged by a methylene-like

H-C-CH₃ group. The methylenic unit is oriented such that its hydrogen ligand [H(7)] extends outward, away from the carborane cage, while the attached methyl ligand [CM(7)] is

Table II. Interatomic Distances (Å)^a

Cage B-B, B-C, and C-C Distances			
B(1)-B(2)	1.786(5)	B(5)-B(6)	1.751(5)
B(1)-B(3)	1.725(5)	B(5)-C(10)	1.745(4)
B(1)-B(4)	1.728(5)	B(5)-B(11)	1.757(4)
B(1)-B(5)	1.778(5)	B(6)-B(11)	1.750(5)
B(1)-B(6)	1.778(5)	B(6)-B(12)	1.769(4)
B(2)-B(3)	1.810(5)	C(7)-C(8)	1.533(4)
B(2)-B(6)	1.751(5)	C(7)-B(12)	1.611(4)
B(2)-C(7)	2.387(5)	C(7)-CM(7)	1.517(4)
B(2)-C(8)	2.083(4)	C(8)-C(9)	1.543(4)
B(2)-B(12)	1.964(5)	C(8)-CM(8)	1.508(4)
B(3)-B(4)	1.755(5)	C(9)-C(10)	1.565(4)
B(3)-C(8)	1.712(4)	C(9)-CM(9)	1.510(4)
B(3)-C(9)	1.780(5)	C(10)-B(11)	1.626(4)
B(4)-B(5)	1.724(5)	C(10)-CM(10)	1.541(4)
B(4)-C(9)	1.733(4)	B(11)-8(12)	1.769(5)
B(4)-C(10)	1.759(5)	B(12)-CP(13)	1.593(4)
B-H Distances			
B(1)-H(1)	1.00(5)	B(5)-H(5)	1.09(5)
B(2)-H(2)	1.09(5)	B(6)-H(6)	1.13(5)
B(3)-H(3)	1.03(5)	B(11)-H(11)	1.16(5)
B(4)-H(4)	1.06(5)	⟨B-H⟩	1.08
Cage C-H and Methyl Distances			
C(7)-H(7)	0.95(5)	CM(9)-H(9A)	1.09(5)
CM(7)-H(7A)	0.94(5)	CM(9)-H(9B)	1.00(5)
CM(7)-H(7B)	1.05(5)	CM(9)-H(9C)	1.08(5)
CM(7)-H(7C)	0.92(5)	CM(10)-H(10A)	1.04(5)
CM(8)-H(8A)	1.07(5)	CM(10)-H(10B)	1.11(5)
CM(8)-H(8B)	1.04(5)	CM(10)-H(10C)	0.93(5)
CM(8)-H(8C)	1.02(5)	⟨CM-H⟩	1.02
Cobaltocenium Distances			
Co-CP(13)	2.107(3)	CP(18)-CP(19)	1.422(4)
Co-CP(14)	2.026(3)	CP(19)-CP(20)	1.419(5)
Co-CP(15)	2.026(3)	CP(20)-CP(21)	1.391(5)
Co-CP(16)	2.020(3)	CP(21)-CP(22)	1.398(5)
Co-CP(17)	2.038(3)	CP(22)-CP(18)	1.418(5)
Co-CP(18)	2.044(3)	CP(14)-H(14)	0.97(5)
Co-CP(19)	2.035(3)	CP(15)-H(15)	1.12(5)
Co-CP(20)	2.037(3)	CP(16)-H(16)	0.90(5)
Co-CP(21)	2.050(3)	CP(17)-H(17)	1.01(5)
Co-CP(22)	2.043(3)	CP(18)-H(18)	0.99(5)
CP(13)-CP(14)	1.449(4)	CP(19)-H(19)	0.90(5)
CP(14)-CP(15)	1.428(4)	CP(20)-H(20)	0.87(5)
CP(15)-CP(16)	1.398(5)	CP(21)-H(21)	1.00(5)
CP(16)-CP(17)	1.418(4)	CP(22)-H(22)	1.05(5)
CP(17)-CP(13)	1.431(4)	⟨CP-H⟩	0.98

^a Distances shown for molecule 1. Corresponding distances for molecules 2 and 3 are identical within two standard deviations.

Table III. Selected Bond Angles (deg)^a

B(2)-B(1)-B(3)	62.0(2)	C(12)-C(7)-H(7)	110.8(5)
B(2)-B(1)-B(6)	58.8(2)	CM(7)-C(7)-H(7)	105.0(5)
B(3)-B(1)-B(4)	61.1(2)	B(2)-C(8)-8(3)	56.0(2)
B(4)-B(1)-B(5)	58.9(2)	B(2)-C(8)-C(7)	81.1(2)
B(5)-B(1)-B(6)	59.0(2)	B(2)-C(8)-CM(8)	125.5(3)
B(1)-B(2)-B(3)	57.3(2)	B(3)-C(8)-C(9)	66.1(2)
B(1)-B(2)-B(6)	60.4(2)	B(3)-C(8)-CM(8)	107.3(3)
B(3)-B(2)-C(8)	51.6(2)	C(7)-C(8)-C(9)	115.0(3)
B(6)-B(2)-B(12)	56.5(2)	C(7)-C(8)-CM(8)	110.8(2)
C(8)-B(2)-B(12)	77.0(2)	C(9)-C(8)-CM(8)	117.1(3)
B(1)-B(3)-B(2)	60.7(2)	B(3)-C(9)-B(4)	59.9(2)
B(1)-B(3)-B(4)	59.6(2)	B(3)-C(9)-C(8)	61.5(2)
B(2)-B(3)-C(8)	72.4(2)	B(3)-C(9)-CM(9)	122.7(3)
B(4)-B(3)-C(9)	58.7(2)	B(4)-C(9)-C(10)	64.2(2)
C(8)-B(3)-C(9)	52.4(2)	B(4)-C(9)-CM(9)	113.5(2)
B(1)-B(4)-B(3)	59.4(2)	C(8)-C(9)-C(10)	116.0(2)
B(1)-B(4)-B(5)	62.0(2)	C(8)-C(9)-CM(9)	117.3(3)
B(3)-B(4)-C(9)	61.4(2)	C(10)-C(9)-CM(9)	118.6(3)
B(5)-B(4)-C(10)	60.1(2)	B(4)-C(10)-B(5)	59.0(2)
C(9)-B(4)-C(10)	53.2(2)	B(4)-C(10)-C(9)	62.5(2)
B(1)-B(5)-B(4)	59.1(2)	B(4)-C(10)-CM(10)	116.8(2)
B(1)-B(5)-B(6)	60.5(2)	B(5)-C(10)-B(11)	62.7(2)
B(4)-B(5)-B(10)	60.9(2)	B(5)-C(10)-CM(10)	116.6(3)
B(6)-B(5)-B(11)	59.8(2)	C(9)-C(10)-B(11)	121.9(3)
C(10)-B(5)-B(11)	55.3(2)	C(9)-C(10)-CM(10)	115.9(3)
B(1)-B(6)-B(2)	60.8(2)	B(11)-C(10)-CM(10)	115.4(3)
B(1)-B(6)-B(5)	60.5(2)	B(5)-B(11)-B(6)	59.9(2)
B(2)-B(6)-B(12)	67.8(2)	B(5)-B(11)-C(10)	62.0(2)
B(5)-B(6)-B(11)	60.2(2)	B(6)-B(11)-B(12)	60.4(2)
B(11)-B(6)-B(12)	60.3(2)	C(10)-B(11)-B(12)	112.4(3)
C(8)-C(7)-B(12)	106.5(2)	B(2)-B(12)-B(6)	55.7(2)
C(8)-C(7)-CM(7)	111.3(2)	B(2)-B(12)-C(7)	83.2(2)
C(12)-C(7)-CM(7)	117.0(3)	B(2)-B(12)-CP(13)	120.5(2)
B(8)-C(7)-H(7)	105.8(5)	B(6)-B(12)-B(11)	59.3(2)
B(6)-B(12)-CP(13)	110.3(2)	CP(14)-CP(15)-CP(16)	107.2(3)
C(7)-B(12)-B(11)	107.2(2)	CP(15)-CP(16)-CP(17)	108.8(3)
C(7)-B(12)-CP(13)	116.0(2)	CP(16)-CP(17)-CP(13)	109.7(3)
B(11)-B(12)-CP(13)	123.0(3)	CP(19)-CP(18)-CP(22)	106.8(8)
B(12)-CP(13)-CP(14)	126.0(3)	CP(18)-CP(19)-CP(20)	107.8(3)
B(12)-CP(13)-CP(17)	129.4(3)	CP(19)-CP(20)-CP(21)	108.1(3)
CP(14)-CP(13)-CP(17)	104.6(2)	CP(20)-CP(21)-CP(22)	108.7(3)
CP(13)-CP(14)-CP(15)	109.6(3)	CP(21)-CP(22)-CP(18)	108.6(3)

^a Angles shown for molecule 1. Corresponding angles for molecules 2 and 3 are identical within two standard deviations.

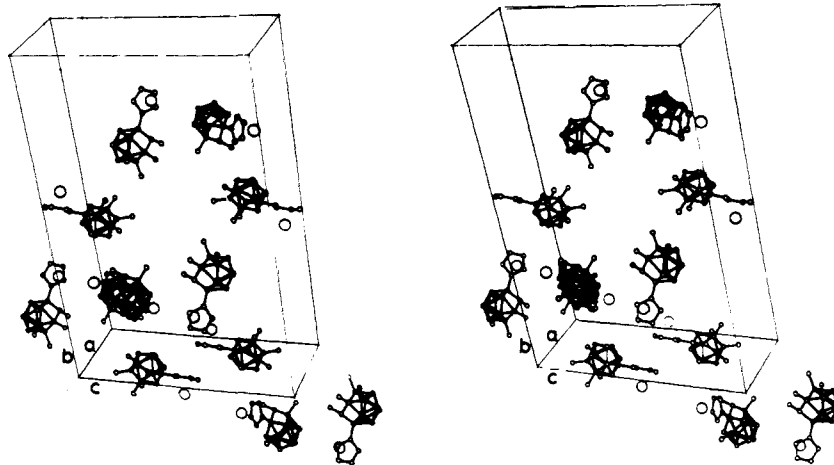


Figure 3. Stereoview of unit cell contents, with one C₅H₅ ring in each molecule omitted for clarity.

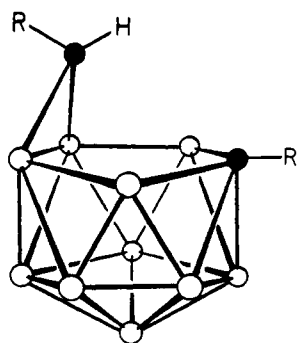


Figure 4. Structure of the R₂C₂B₁₀H₁₁⁻ ions (R = CH₃,⁶ C₆H₅⁷). Black and white circles indicate carbon and boron atoms, respectively; framework hydrogens are not shown.

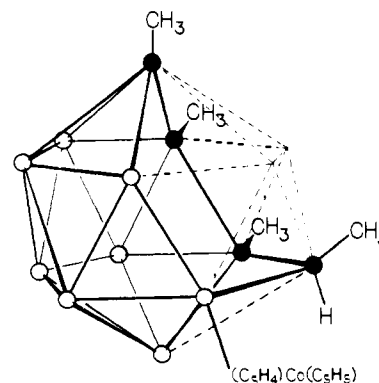


Figure 5. Geometry of the C₄B₈ cage in the title compound, shown as a fragment of a 14-vertex closo polyhedron. The enantiomer depicted is different from the one shown in Figures 1 and 2.

Table IV. Selected Intramolecular Planes^{a, b}

atom	deviation	atom	deviation
Plane 1: C(8), C(9), C(10), B(11), B(12)			
$-0.1812x + 0.1427y - 0.9730z + 5.1099 = 0$			
C(8)	-0.016	B(11)	0.014
C(9)	0.031	B(12)	0.001
C(10)	-0.030	C(7)	-0.834
Plane 2: CP(13), CP(14), CP(15), CP(16), CP(17)			
$-0.6452x + 0.3792y - 0.6632z + 0.0926 = 0$			
CP(13)	0.017	CP(17)	-0.013
CP(14)	-0.015	B(12)	0.043
CP(15)	0.008	Co	-1.645
CP(16)	0.004		
Plane 3: CP(18), CP(19), CP(20), CP(21), CP(22)			
$-0.6485x + 0.3831y - 0.6578z + 3.3070 = 0$			
CP(18)	-0.001	CP(21)	-0.004
CP(19)	-0.001	CP(22)	0.003
CP(20)	0.003	Co	1.653

^a Calculated for molecule 1; deviations and angles for corresponding planes in molecules 2 and 3 are not significantly different. ^b Angles: planes 1 and 2, 35.3°; planes 1 and 3, 35.7°; planes 2 and 3, 0.43°.

above the open face. This latter feature is one of the more striking aspects of the structure, and we comment on it further below. The cobaltocenium substituent is attached to B(12) and appears unremarkable; there is no apparent steric interaction between it and the carborane cage. The B(2)-B(12) and B(2)-C(8) distances are unusually long [1.964 (5) and 2.083 (4) Å, respectively], but must be considered bonding. All other B-B, B-C, and C-C bond lengths in the molecule appear normal.

Comparison with the (CH₃)₂C₂B₁₀H₁₁⁻ and (C₆H₅)₂C₂B₁₀H₁₁⁻ Ions. The dicarbon carborane dianion, C₂B₁₀H₁₂²⁻, and its monoprotonated derivative C₂B₁₀H₁₃⁻ have not been structurally characterized, but crystal structure determinations on the C,C'-dimethyl⁶ and C,C'-diphenyl⁷ derivatives of the latter system revealed the cage structure shown in Figure 4. These molecules contain bridging -CHR- groups and in that respect resemble the tetracarbon species reported here, but there are two major differences. First, in the R₂C₂B₁₀H₁₁⁻ systems the methylenic carbon bridges two boron atoms which are bonded to each other [1.85 (2) Å] whereas in the present molecule the bridged atoms are non-bonded, as already noted. This observation is consistent with the fact that the R₂C₂B₁₀H₁₁⁻ species are formally 28-electron nido systems²⁰ analogous to B₁₂H₁₂⁴⁻, while the (CH₃)₄-C₄B₈H₈²⁻ derivative described here is a 30-electron arachno cage corresponding to B₁₂H₁₂⁶⁻; as expected, the 30-electron species has the more open structure. This is clearly seen in

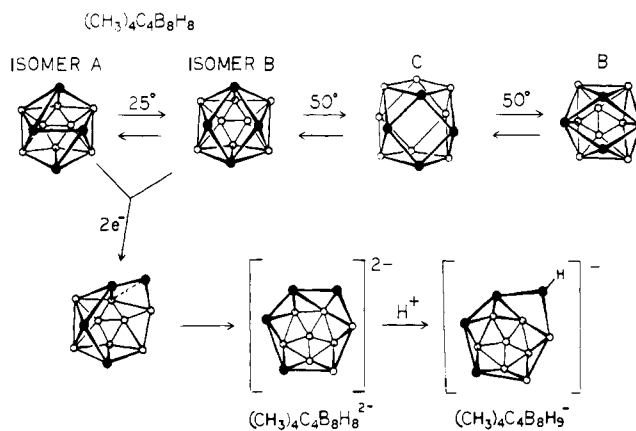


Figure 6. Proposed scheme for the interconversion of neutral (CH₃)₄-C₄B₈H₈ isomers A and B, the fluxional rearrangement of B at 50 °C, and the formation of the (CH₃)₄C₄B₈H₈²⁻ and (CH₃)₄C₄B₈H₉⁻ ions. The structures of isomer A⁸ and the (CH₃)₄C₄B₈H₉⁻ ions²⁶ are established; geometries of the other species are postulated from NMR evidence. ●, CCH₃; ○, BH.

Figure 5, where the molecule is depicted as a 14-vertex closo polyhedron²¹ with two missing vertices, precisely in line with the general description of arachno cages as given by several authors.^{5,14}

The other obvious difference between the R₂C₂B₁₀H₁₁⁻ structures and the (CH₃)₄C₄B₈H₈²⁻ derivative is in the orientation of the bridging R-C-H groups with respect to the cage. The placement of the methyl group over the open face in the C₄B₈ system, with the unique hydrogen directed away from the cage (Figures 1 and 2), probably reflects the mode of H⁺ attack on the (CH₃)₄C₄B₈H₈²⁻ ion. We think it likely that the dianion, which lacks an "extra" proton, has the structure shown at the bottom center of Figure 6, in which all four carbon atoms are fully bonded into the carborane framework. This is assumed since removal of the "extra" proton from the bridging carbon atom in the (CH₃)₄C₄B₈H₉⁻ ion would leave that carbon coordinatively unsaturated, inducing it to move into the cage.

The fact that protonation of the R₂C₂B₁₀H₁₂²⁻ and (CH₃)₄C₄B₈H₈²⁻ ions in both cases occurs at a carbon atom rather than at a boron-boron edge on the open face can be explained in terms of relief of valence angle strain in the cage by movement of a carbon atom from a framework vertex into a bridging location. Formation of a bridging R-C-H group in each case allows the remainder of the cage to adopt, or ap-

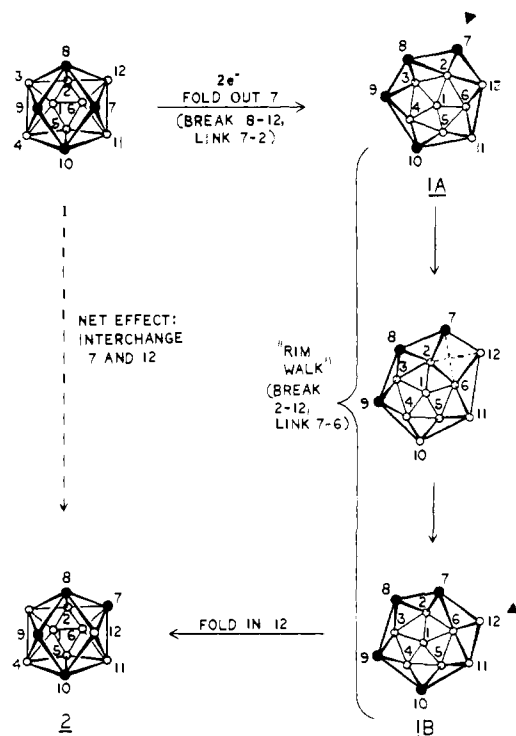


Figure 7. Proposed mechanisms for the fluxional rearrangement of the $(\text{CH}_3)_4\text{C}_4\text{B}_8\text{H}_8^{2-}$ framework. Isomer **1A** corresponds to the geometry established for $(\text{C}_3\text{H}_5)\text{Co}(\text{C}_5\text{H}_4)^+(\text{CH}_3)_4\text{C}_4\text{B}_8\text{H}_8^-$; isomer **1B** is similar but the unique low-coordinate position (marked by wedges in both structures) is occupied by a BH instead of a CCH_3 unit.

proach, the highly favored geometry of an icosahedral fragment.

Structural Relationship of the $(\text{CH}_3)_4\text{C}_4\text{B}_8\text{H}_8$ Isomers and the $(\text{CH}_3)_4\text{C}_4\text{B}_8\text{H}_8^{2-}$ Ion. The geometry of neutral $(\text{CH}_3)_4\text{C}_4\text{B}_8\text{H}_8$ in the solid state (isomer A) was determined crystallographically several years ago⁸ and is shown in Figure 6 together with our proposed structure²⁴ for isomer B; the latter species exists in equilibrium with A in solution, but reverts to A on evaporation of solvent.²⁵ The suggested geometry of B is consistent with²⁵ (1) the ^1H and ^{11}B FT NMR spectra, which indicate either C_3 or C_2 point group symmetry; (2) the facile interconversion of A and B even in cold solvents, which requires a low activation energy barrier; (3) the observed equivalence of all four C- CH_3 groups in the ^1H spectrum of B at 50 $^\circ\text{C}$, which can be explained in terms of a cube-octahedral time-averaged intermediate structure (C), also shown in Figure 6.

The conversion of either A or B to the $(\text{CH}_3)_4\text{C}_4\text{B}_8\text{H}_8^{2-}$ dianion can be readily envisioned as a cage-opening process, depicted in Figure 6. While the mechanistic details are unclear, the net result is movement of one C- CH_3 group to the rim, creating a large open face. When the dianion is subsequently treated with HCl to form $(\text{CH}_3)_4\text{C}_4\text{B}_8\text{H}_9^-$, the proton attack occurs at C(7), converting it into a bridging $\text{CH}_3\text{-C-H}$ group as observed in the cobaltocenium derivative reported here.²⁶

The ^{11}B FT NMR spectrum of $\text{Na}_2(\text{CH}_3)_4\text{C}_4\text{B}_8\text{H}_8$ in CD_3CN at room temperature exhibits four equal-area resonances, which for a static structure would imply twofold or mirror symmetry.⁹ However, the pattern of metallocarboranes obtained from reactions of the metal ions with the $(\text{CH}_3)_4\text{C}_4\text{B}_8\text{H}_8^{2-}$ dianion (discussed below) strongly suggests that the dianion exists in solution as a mixture of rapidly interconverting isomers. Direct study of this proposed fluxional behavior has not been possible due to solubility problems which

prevent observation of low-temperature spectra of the salt, but a scheme which allows facile interconversion of dianion structures is suggested in Figure 7. Two kinds of fluxional processes are envisioned, the first of which involves stretching the B(2)-B(12) link in **1A** and forming a B(6)-C(7) bond, as in **1B** (a "diamond-square-diamond"²⁷ rearrangement); this places B(12) in the unique low-coordinate vertex on the open face, a situation originally occupied by C(7). Repetition of this process on **1B** [i.e., breaking B(6)-B(11) and linking B(5)-B(12)] converts B(11) into a low-coordinate vertex, and in this manner each of the rim atoms (7, 8, 9, 10, 11, 12) can adopt the low-coordinate role in turn. It is convenient to refer to this kind of fluxional behavior as "rim walking".

The second proposed rearrangement process consists of folding the low-coordinate group (whatever it may be at a given moment) into the open face to generate an intermediate with quasi-icosahedral geometry, as illustrated in the conversion of **1B** to **2** at the bottom of Figure 7. This "fold-in" process is, of course, schematically the reverse of the "fold-out" mechanism at the top of the figure, except that different atoms are involved. It seems not unreasonable that the $(\text{CH}_3)_4\text{C}_4\text{B}_8\text{H}_8^{2-}$ dianion would alternate between open and quasi-closed structures as shown, since there would be two opposing driving forces at work: the inherent stability and symmetry of the icosahedron, and the presence of extra electrons beyond the optimum number of 26 in the skeletal molecular orbitals, which would tend to favor cage opening.

The fold-out \rightarrow "rim walk" \rightarrow fold-in sequence in Figure 7 interchanges C(7) and B(12) in the original quasi-icosahedral cage. Since the nonbonded interaction in such a cage could in principle occur along any edge of the original polyhedron, this rearrangement sequence is capable of interchanging any two adjacent atoms on the polyhedral surface; in such a case the $(\text{CH}_3)_4\text{C}_4\text{B}_8\text{H}_8^{2-}$ ion in solution would exist as a mixture of different isomers, so that insertion of metal groups would generate a variety of structurally diverse metallocarboranes. Such metallocarborane mixtures are indeed observed,^{1b,9} and the structures of the isolated metallocarborane products supply clues to the geometries of the $(\text{CH}_3)_4\text{C}_4\text{B}_8\text{H}_8^{2-}$ dianions, as we show in the following section.

Formation of Iron Metallocarboranes from $(\text{CH}_3)_4\text{C}_4\text{B}_8\text{H}_8^{2-}$. The proposed stereochemical behavior of the $(\text{CH}_3)_4\text{C}_4\text{B}_8\text{H}_8^{2-}$ dianion in solution as depicted in Figure 7 allows us to deal with the observed^{1b,9} structures of metallocarboranes which form by metal ion insertion into the cage. In earlier work⁹ it was found that the reaction of the dianion with FeCl_2 and NaC_5H_5 in THF at room temperature generates $(\eta^5\text{-C}_5\text{H}_5)\text{Fe}(\text{CH}_3)_4\text{C}_4\text{B}_7\text{H}_8$ and at least four isomers of $(\eta^5\text{-C}_5\text{H}_5)_2\text{Fe}_2(\text{CH}_3)_4\text{C}_4\text{B}_8\text{H}_8$. The structures of the FeC_4B_7 and two of the $\text{Fe}_2\text{C}_4\text{B}_8$ species were determined crystallographically⁹ and found to contain highly irregular, unprecedented cage geometries (Figure 8, structures **5**, **6**, and **7**) in which the distribution of skeletal carbon atoms appeared to follow no simple pattern.

Inspection of models and diagrams of atomic connectivity in these molecules satisfies us that there are no energetically reasonable *direct* pathways for the conversion of the known $(\text{CH}_3)_4\text{C}_4\text{B}_8\text{H}_8^{2-}$ isomer (Figure 6) to any of the three ferrocenanes **5**, **6**, and **7**, or for the interconversion of **6** and **7**. However, by making use of the proposed fluxionality of the $(\text{CH}_3)_4\text{C}_4\text{B}_8\text{H}_8^{2-}$ anion as outlined in Figure 7, it is possible to account for the observed structures. We propose that two parallel but separate processes are involved in the metallocarborane formation (Figure 8). One route entails the insertion of a $(\text{C}_5\text{H}_5)\text{Fe}^+$ unit into the open face of a rearranged $(\text{CH}_3)_4\text{C}_4\text{B}_8\text{H}_8^{2-}$ dianion (**3**) to form a 13-vertex $(\eta^5\text{-C}_5\text{H}_5)\text{Fe}(\text{CH}_3)_4\text{C}_4\text{B}_8\text{H}_8^-$ monoanion **4** (not isolated),²⁸ which is a 30-electron ($2n + 4$) system and should be nido, as shown. Loss of B(4) from **4** with retention of its hydrogen atom as a B-H-B bridge yields the structurally characterized⁹ complex **5**. In-

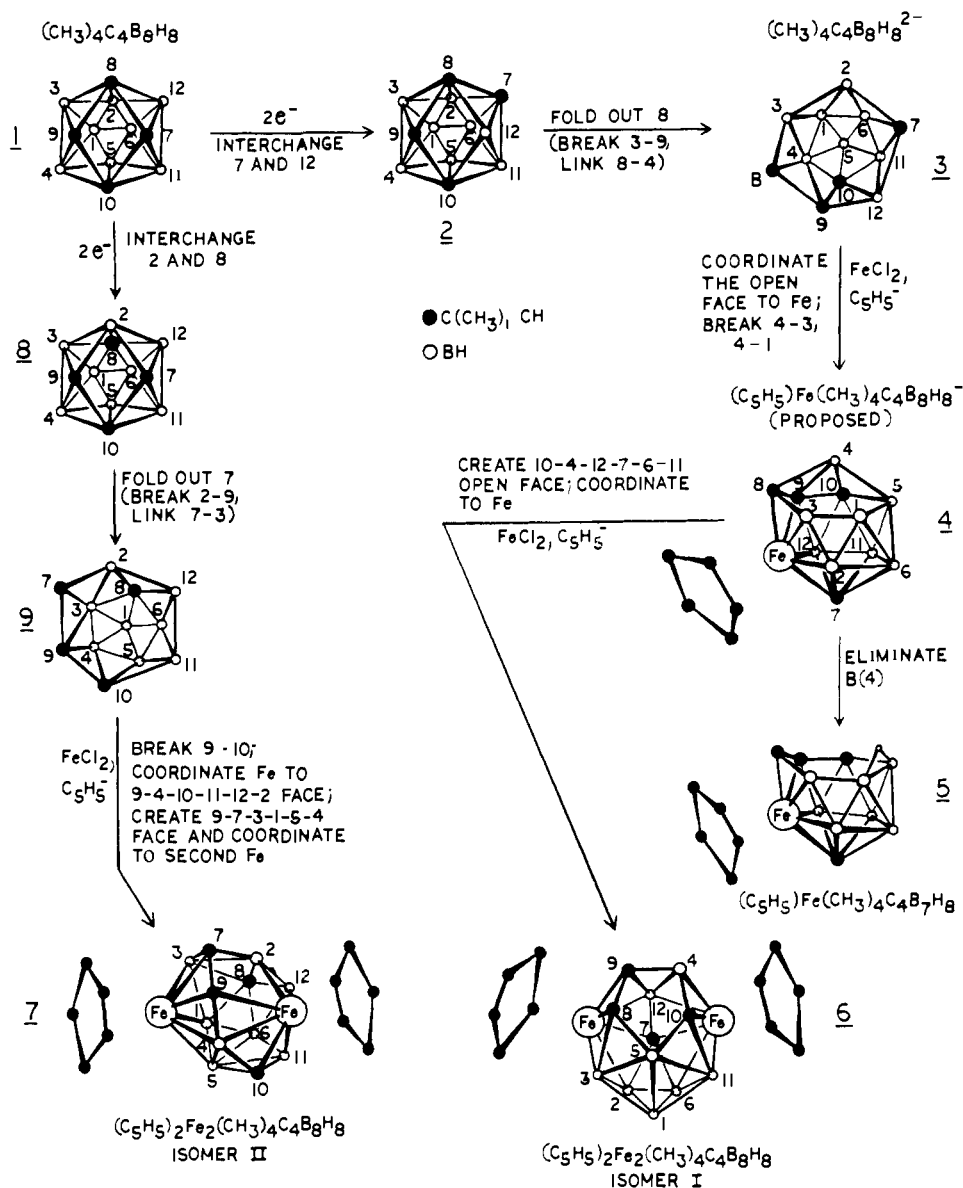


Figure 8. Proposed mechanisms for the formation of the ferracarboranes 5, 6, and 7, via isomers of the $(\text{CH}_3)_4\text{C}_4\text{B}_8\text{H}_8^{2-}$ dianion which can form by processes of the kind illustrated in Figure 7. The structures of the end products 5, 6, and 7 are established.^{9,23}

sertion of a $(\text{C}_5\text{H}_5)\text{Fe}^+$ into 4, with some minor atomic movement in the framework to accommodate the second metal atom, produces the known $(\eta^5\text{-C}_5\text{H}_5)_2\text{Fe}_2(\text{CH}_3)_4\text{C}_4\text{B}_8\text{H}_8$, isomer I (6).

The insertion of two $(\text{C}_5\text{H}_5)\text{Fe}^+$ groups into a different rearranged isomer of $(\text{CH}_3)_4\text{C}_4\text{B}_8\text{H}_8^{2-}$ (9) generates $(\eta^5\text{-C}_5\text{H}_5)_2\text{Fe}_2(\text{CH}_3)_4\text{C}_4\text{B}_8\text{H}_8$, isomer II (7), in about the same number of steps as was required for isomer I. The postulated existence of several different isomers of the dianion would lead one to expect still other ferracarborane products, since presumably these other forms of the dianion would also be susceptible to metal insertion. In fact, at least four isomers of $(\eta^5\text{-C}_5\text{H}_5)_2\text{Fe}_2(\text{CH}_3)_4\text{C}_4\text{B}_8\text{H}_8$ are known to form in the reaction.⁹

Conclusions

The proposed mechanisms for metallocarborane formation in Figures 7 and 8 are at present supported to the extent that the structures of neutral $(\text{CH}_3)_4\text{C}_4\text{B}_8\text{H}_8$ (isomer A),⁸ a cobaltocenium derivative of $(\text{CH}_3)_4\text{C}_4\text{B}_8\text{H}_8^{2-}$, and three isolated

ferracarborane complexes²³ have been established. In addition, we have determined the structures of a cobalt species, $(\eta^5\text{-C}_5\text{H}_5)\text{Co}(\text{CH}_3)_4\text{C}_4\text{B}_7\text{H}_7$ (isomer II),¹³ and a nickel complex, $[(\text{C}_6\text{H}_5)_2\text{PCH}_2]_2\text{Ni}(\text{CH}_3)_4\text{C}_4\text{B}_8\text{H}_8$ (isomer I),²⁹ which were obtained^{1b,9} from the $(\text{CH}_3)_4\text{C}_4\text{B}_8\text{H}_8^{2-}$ dianion; these very recent findings provide still more evidence for the existence of isomers of the dianion in solution. The stereochemical details of these processes are certainly open to question, and other mechanisms can by no means be excluded, although alternative routes we have considered tend to be either longer or more complex, or to involve energetically less likely cage rearrangements. At the least, the structures thus far determined and the mechanistic ideas suggested herein provide a framework against which subsequent work in tetracarborane stereochemistry can be viewed. Structural and synthetic investigations in this area are continuing in our laboratory.

Acknowledgment. This work was supported by the National Science Foundation, Grant CHE 76-04491, and the Office of Naval Research.

Supplementary Material Available: A listing of observed and calculated structure factors and a table of positional and thermal parameters (32 pages). Ordering information is given on any current masthead page.

References and Notes

- (1) (a) Tetracarbon Metallocarboranes. 8. (b) For part 7, see W. M. Maxwell and R. N. Grimes, *Inorg. Chem.*, in press.
- (2) W. N. Lipscomb, "Boron Hydrides", W. A. Benjamin, New York, 1963, and references cited therein.
- (3) H. C. Longuet-Higgins and M. de V. Roberts, *Proc. R. Soc. London, Ser. A*, **224**, 336 (1954); **230**, 110 (1955).
- (4) E. B. Moore, Jr., L. L. Lohr, Jr., and W. N. Lipscomb, *J. Chem. Phys.*, **35**, 1329 (1961).
- (5) Procedures for counting framework electrons in polyhedral cages are given by (a) K. Wade, *Adv. Inorg. Chem. Radiochem.*, **18**, 1 (1976); (b) D. M. P. Mingos, *Nature (London), Phys. Sci.*, **236**, 99 (1972); (c) R. W. Rudolph, *Acc. Chem. Res.*, **9**, 446 (1976).
- (6) M. R. Churchill and B. G. DeBoer, *Inorg. Chem.*, **12**, 2674 (1973).
- (7) E. I. Tolpin and W. N. Lipscomb, *Inorg. Chem.*, **12**, 2257 (1973).
- (8) D. P. Freyberg, R. Weiss, E. Sinn, and R. N. Grimes, *Inorg. Chem.*, **16**, 1847 (1977).
- (9) W. M. Maxwell, R. F. Bryan, and R. N. Grimes, *J. Am. Chem. Soc.*, **99**, 4008 (1977).
- (10) K.-S. Wong, J. R. Bowser, J. R. Pipal, and R. N. Grimes, *J. Am. Chem. Soc.*, **100**, 5045 (1978).
- (11) J. R. Pipal and R. N. Grimes, *Inorg. Chem.*, in press.
- (12) J. R. Pipal and R. N. Grimes, *J. Am. Chem. Soc.*, **100**, 3083 (1978).
- (13) E. Sinn, J. R. Pipal, and R. N. Grimes, to be submitted for publication.
- (14) R. E. Williams, *Inorg. Chem.*, **10**, 210 (1971).
- (15) P. W. R. Corfield, R. J. Doedens, and J. A. Ibers, *Inorg. Chem.*, **6**, 197 (1967).
- (16) D. T. Cromer and J. T. Waber, "International Tables for X-ray Crystallography", Vol. IV, Kynoch Press, Birmingham, England, 1974.
- (17) R. F. Stewart, E. R. Davidson, and W. T. Simpson, *J. Chem. Phys.*, **42**, 3175 (1965).
- (18) D. T. Cromer and J. A. Ibers, ref. 16.
- (19) D. P. Freyberg, G. M. Mockler, and E. Sinn, *J. Chem. Soc., Dalton Trans.*, 447 (1976).
- (20) Nido cages contain $2n + 4$ skeletal electrons (where n is the number of framework atoms) and normally adopt open geometry based on a closed polyhedral (closo) cage with one missing vertex. Arachno systems have $2n + 6$ skeletal electrons and resemble closo polyhedra with two missing vertices.^{5,14}
- (21) The prototype closo 14-vertex polyhedron is a bicapped hexagonal antiprism, of which the only structurally established example is $(\eta^5\text{-C}_5\text{H}_5)_2\text{-Fe}_2(\text{CH}_3)_4\text{C}_4\text{B}_8\text{H}_8$ (isomer VIII).^{22,23}
- (22) J. R. Pipal and R. N. Grimes, *Inorg. Chem.*, **17**, 6 (1978).
- (23) W. M. Maxwell, R. Weiss, E. Sinn, and R. N. Grimes, *J. Am. Chem. Soc.*, **99**, 4016 (1977).
- (24) Early structural proposals,²⁵ made prior to the crystallographic studies, speculated that A and B had open and closed geometries, respectively. Subsequently, the observed⁸ structure of A turned out to be very similar to that originally proposed for B.
- (25) W. M. Maxwell, V. R. Miller, and R. N. Grimes, *Inorg. Chem.*, **15**, 1343 (1976).
- (26) It is assumed that the cobaltocenium group does not appreciably influence the observed geometry of the carborane anion.
- (27) W. N. Lipscomb, *Science*, **153**, 373 (1966).
- (28) A neutral $(\eta^5\text{-C}_5\text{H}_5)_2\text{Co}(\text{CH}_3)_4\text{C}_4\text{B}_8\text{H}_8$ species which is isoelectronic with 4 has been isolated and characterized from the reaction of CoCl_2 and NaC_5H_5 ; see ref 1b.
- (29) E. Sinn and R. N. Grimes, to be submitted for publication.

Blue Copper Proteins. Synthesis, Chemistry, and Spectroscopy of $\text{Cu}^{\text{I}}\text{N}_3(\text{SR})$ and $\text{Cu}^{\text{II}}\text{N}_3(\text{SR})$ Active Site Approximations. Crystal Structure of Potassium *p*-Nitrobenzenethiolato(hydrotris(3,5-dimethyl-1-pyrazolyl)-borato)cuprate(I) Diacetone, $\text{K}[\text{Cu}(\text{HB}(3,5\text{-Me}_2\text{pz})_3)\text{-}(\text{SC}_6\text{H}_4\text{NO}_2)]\cdot 2\text{C}_3\text{H}_6\text{O}$

Jeffery S. Thompson, Tobin J. Marks,* and James A. Ibers*

Contribution from the Department of Chemistry and the Materials Research Center, Northwestern University, Evanston, Illinois 60201. Received September 7, 1978

Abstract: The cuprous complexes $\text{K}[\text{Cu}(\text{HB}(3,5\text{-Me}_2\text{pz})_3)(\text{SR})]$ ($\text{SR} = p$ -nitrobenzenethiolate or *O*-ethylcysteinate; $\text{HB}(3,5\text{-Me}_2\text{pz})_3 = \text{hydrotris}(3,5\text{-dimethyl-1-pyrazolyl})\text{borate}$) can be prepared by the reaction of $\text{Cu}(\text{SR})$ or $[\text{Cu}(\text{SR})]\text{-}(\text{ClO}_4)$ with $\text{KHB}(3,5\text{-Me}_2\text{pz})_3$ at room temperature. The structure of the complex with $\text{SR} = p$ -nitrobenzenethiolate has been determined by X-ray diffraction methods. The complex crystallizes in the triclinic space group $C_1^1 - P\bar{1}$ with two molecules in a unit cell of dimensions $a = 10.60$ (2) Å, $b = 18.17$ (4) Å, $c = 10.33$ (4) Å, $\alpha = 93.57$ (5)°, $\beta = 116.20$ (7)°, and $\gamma = 71.89$ (5)°. Least-squares refinement of the 117 variables has led to a value of the conventional *R* index (on *F*) of 0.092 for 678 independent reflections having $F_o^2 > 3\sigma(F_o^2)$. The geometry about the Cu^{I} atom, which is coordinated to three nitrogen atoms and one sulfur atom, is trigonally distorted tetrahedral. The cupric complexes $\text{Cu}(\text{HB}(3,5\text{-Me}_2\text{pz})_3)(\text{SR})$ ($\text{SR} = p$ -nitrobenzenethiolate or *O*-ethylcysteinate) have been prepared by the reaction of $\text{KHB}(3,5\text{-Me}_2\text{pz})_3$ with the corresponding $[\text{Cu}(\text{SR})]\text{-}(\text{ClO}_4)$ derivatives at -78 °C. UV-visible, laser Raman, and EPR data are used to show that the Cu^{II} complexes have a very similar structure to that of the Cu^{I} complex characterized by X-ray diffraction methods. The Cu^{II} complex $\text{Cu}(\text{HB}(3,5\text{-Me}_2\text{pz})_3)(\text{OR})$ ($\text{OR} = p$ -nitrobenzenephenolate, $\text{OC}_6\text{H}_4\text{NO}_2$) was prepared by the reaction of $\text{NaOC}_6\text{H}_4\text{NO}_2\cdot 2\text{H}_2\text{O}$ with $\text{CuBr}(\text{HB}(3,5\text{-Me}_2\text{pz})_3)$ in tetrahydrofuran at room temperature. The UV-visible, laser Raman, and EPR data for this complex are used in the interpretation of the spectra of the $\text{Cu}^{\text{I}}\text{N}_3(\text{SR})$ and $\text{Cu}^{\text{II}}\text{N}_3(\text{SR})$ complexes. The spectral properties of the $\text{Cu}^{\text{II}}\text{N}_3(\text{SR})$ complexes are similar to those of the blue (type 1) copper proteins and allow certain definite conclusions to be drawn concerning the origin of the distinctive UV-visible, resonance Raman, and EPR spectral features of the proteins.

A variety of copper-containing proteins, some of which play important roles in electron transport and/or oxidase activity, contain a highly unusual form of copper ion.¹⁻⁶ The "blue" or "type 1" binding sites of metalloproteins such as azurin, plastocyanin, stellacyanin, umecyanin, cytochrome oxidase, ascorbate oxidase, laccase, and ceruloplasmin confer

upon the copper ion chemical and spectral properties that are unique among copper complexes.¹⁻⁶ These properties include generally high redox potentials compared with the $\text{Cu}^{\text{II}}/\text{Cu}^{\text{I}}$ couple in aqueous solution (i.e., the cuprous form of the type 1 core is unusually stable) and distinctive spectral features. The oxidized, cupric forms of the type 1 proteins display very in-